Available online at www.sciencedirect.com
SCIENCE DIRECT®
Journal of Catalysis 221 (2004) 510–522
JOURNAL OF CATALYSIS
www.elsevier.com/locate/jcat

Atomic-scale insight into structure and morphology changes of MoS_2 nanoclusters in hydrotreating catalysts

J.V. Lauritsen,[a] M.V. Bollinger,[b] E. Lægsgaard,[a] K.W. Jacobsen,[b] J.K. Nørskov,[b] B.S. Clausen,[c] H. Topsøe,[c] and F. Besenbacher[a,*]

[a] *Department of Physics and Astronomy, Interdisciplinary Nanoscience Center and Center for Atomic-scale Materials Physics, University of Aarhus, DK-8000 Aarhus C, Denmark*

[b] *Department of Physics and Center for Atomic-scale Materials Physics, Technical University of Denmark, DK-2800 Lyngby, Denmark*

[c] *Haldor Topsøe A/S, Nymøllevej 55, DK-2800 Lyngby, Denmark*

Received 4 June 2003; revised 12 September 2003; accepted 12 September 2003

Abstract

High-resolution scanning tunneling microscopy (STM) is used in combination with density-functional theory (DFT) to provide new insight into the morphology and atomic-scale structure of MoS_2 nanoclusters in hydrodesulfurization (HDS) catalysts. Atom-resolved STM images of gold-supported single-layer MoS_2 nanoclusters reveal the first direct evidence that both the detailed atomic-scale structure of the catalytically important edges and the overall morphology of the nanoparticles are sensitive to sulfiding and reaction conditions. Specifically, it is shown that synthesis in $H_2S{:}H_2 = 500$ results in MoS_2 nanoclusters with a triangular morphology, whereas sulfiding in $H_2S{:}H_2 = 0.07$ leads to hexagonally truncated nanoclusters. For both morphologies we identify the exact geometric edge structure of the MoS_2 nanoclusters by comparing the atom-resolved STM images with STM simulations. Whereas the MoS_2 triangles are terminated by dimer-saturated Mo edges, the hexagonal MoS_2 structures exhibit completely different edge structures with a lower sulfur coverage on the Mo edges and S edges with adsorbed S–H groups. A thermodynamic model based on DFT is employed to construct phase diagrams which can predict the stability of different MoS_2 edge structures under different conditions. The present results thus provide new insight into the atomic structure of the HDS catalysts and how it may change with reaction conditions.

Keywords: Hydrodesulfurization; HDS; Model catalyst; Scanning tunneling microscopy; STM; Density-functional theory; Molybdenum disulfide; MoS_2 nanoclusters; Morphology; Dynamics; Edge states; Edge structure

1. Introduction

Molybdenum-based hydrodesulfurization (HDS) catalysts have for many years been among the most important refinery catalysts in service. HDS catalytic reactions comprise reductive hydrogen treatments of fuels to clean up sulfur-containing compounds and the field is presently attracting special attention in view of the new demands for ultralow sulfur content in transport fuels [1–6]. The great interest in HDS catalysts has resulted in numerous investigations of the catalyst and the level of understanding has increased substantially as new and better characterization tools have been developed [7,8]. By applying in situ techniques like extended X-ray absorption fine structure (EXAFS), it has been established [9,10] that the active molybdenum is present as small MoS_2-like nanostructures. Combined adsorption and activity experiments using, e.g., O_2, CO, or NO as probe molecules [11,12] have revealed that the active sites reside at the edges of the MoS_2 structures. It has therefore generally been believed that the creation of sulfur vacancies, or so-called coordinatively unsaturated sites (CUS), at the edges plays a key role and is important for binding of the sulfur-containing molecules, but the exact nature of the active site for HDS has remained unsolved. Spectroscopic data have indicated that S–H groups are present at the MoS_2 edges [13], and it was proposed that the S–H groups may play a role in supplying the hydrogen during HDS. Many of the details of HDS mechanisms have still not been resolved but it has been shown that overall trends in catalytic activities also for promoted catalysts can be explained by

* Corresponding author.
E-mail address: fbe@phys.au.dk (F. Besenbacher).

0021-9517/$ – see front matter
doi:10.1016/j.jcat.2003.09.015

constructing simple models based on the edge dispersion of the MoS_2 phase [12,14–16]. For the industrially important Co (or Ni)-promoted MoS_2 catalysts, it is well established that the MoS_2 edges also play a key role since the activity is dominated by promoter atoms in the so-called Co–Mo–S structures [7,12,17].

In order to continue improving HDS catalysts, a detailed understanding of the MoS_2 clusters, their morphology, edge structures, active sites, and interactions with typical molecules is necessary. Progress in this regard has been slow since the traditional in situ spectroscopic studies of industrial type alumina-supported catalysts have not been able to provide an unequivocal real-space picture of the MoS_2 morphology and the prevailing edge structures. To further advance the understanding of the detailed catalyst structure, new insight has been gained from detailed surface science studies. Recently, the STM has emerged as a new tool to directly image catalytically relevant surface structures on the atomic scale. By studying model systems for catalysts, such investigations [18,19] have helped to solve surface structures with catalytic relevance and have, in particular, emphasized the catalytic importance of edges, kinks, atom vacancies, or other surface defects, which other surface-averaging techniques often fail to discover. Recently, the first successful atom-resolved scanning tunneling microscopy (STM) studies performed on a realistic HDS model catalyst were reported. Using a model system consisting of few-nanometer-wide gold-supported MoS_2 particles, it was shown that the real-space structure of the catalytically active particles could be resolved. Such STM studies have presented the first direct structural information for both unpromoted MoS_2 [20] and promoted Co–Mo–S structures [21], and have recently been used to explore the interaction with thiophene (C_4H_4S) [22]. The studies showed, quite surprisingly, that the unpromoted MoS_2 nanoclusters may exhibit a triangular morphology [20] in contrast to the hexagonal morphology expected for bulk crystals. Such a direct view of the MoS_2 morphology is important, since, in the absence of direct insight, most past HDS catalyst models have assumed a morphology based entirely on bulk properties. The STM results were performed after one type of sulfiding procedure and the results do therefore not allow one to conclude that the triangular morphology will always be the one prevailing after different sulfiding procedures or under different HDS conditions. In fact, preliminary STM results did show that this may not be the case [23]. This is interesting since many results in the literature (see, e.g., [7] and references therein) and early kinetic experiments by Gates and co-workers [24] have indicated that structural changes take place when the reaction conditions are changed.

Recently, theoretical studies using density-functional theory (DFT) have provided new insight into the detailed edge structures and have also addressed the issue of MoS_2 morphology. The results by Byskov et al. [27] suggest that fully sulfided MoS_2 structures may favor the $(10\bar{1}0)$ Mo edges, whereas under more reducing conditions $(\bar{1}010)$ S edges are favored. Further studies have recently been published [28,29], and Schweiger et al. [30] have directly calculated the expected shape of MoS_2 clusters under different conditions. The authors considered different sulfur coverages on the edges, but the possible effect of hydrogen adsorption was not included and the results may therefore not fully represent the actual situation. A number of recent DFT studies have in fact suggested structural changes of the edges due to hydrogen adsorption [26,29,31–36].

In this paper we extend our previous experimental and theoretical treatments in order to observe and understand the variety of MoS_2 structures which may form under different reducing and sulfiding conditions. We have previously shown that a uniform ensemble of highly dispersed, single-layer MoS_2 nanoclusters with an average side length of a few nanometers can be formed by high-temperature sulfidation of Mo initially deposited onto a clean Au(111) single-crystal surface kept in a fully sulfiding atmosphere of H_2S [20]. Here, we take advantage of this recent progress in the synthesis and atomic-scale STM characterization of gold-supported MoS_2 nanoclusters as a suitable HDS model catalyst system, to investigate the morphology and atomic-scale edge structures of single-layer MoS_2 nanoclusters synthesized in varying mixtures of H_2S and H_2. By comparing the atomic-scale images provided by STM with simulated STM images based on DFT calculations of MoS_2 edges, we are able to identify the structure of the MoS_2 nanoclusters and relate their stability to the specific thermodynamic parameters under which they exist. We include in these calculations the possibility of hydrogen adsorption on the MoS_2 edges, and in addition to the effects included in Ref. [31] we consider also the possible influence of the gold model substrate. To model the effect of temperature and gas composition, we use the zero-temperature, zero-pressure DFT results in a thermodynamic model to construct phase diagrams. In terms of this model, it is shown that some of the structures studied under vacuum conditions may represent well the state of the catalyst under realistic reaction conditions.

2. Methods

2.1. Scanning tunneling microscopy

The experiments are performed in a standard ultrahigh vacuum (UHV) chamber with a base pressure below 1×10^{-10} mbar. The system is equipped with standard surface science equipment and a high-resolution STM, capable of resolving the atomic details of close packed surfaces and clusters on a routine basis [38,39].

Highly porous metal oxides, like γ-Al_2O_3, are the preferred supports for the industrial HDS catalysts, but since they are electrically insulating, they cannot be used as substrates for STM measurements. To understand the intrinsic properties of MoS_2 nanoclusters, we therefore employ an inert substrate which interacts weakly with MoS_2. We have

chosen the Au(111) surface as a support for the catalyst model system. H_2S does not adsorb on this surface at temperatures above 160 K [40]; furthermore, the characteristic "herringbone" surface reconstruction of Au(111) [41] provides a regular array of sites which are ideal for the nucleation of deposited metal atoms which facilitates the dispersion submonolayer amounts of Mo into nanoclusters [20,21]. The Au(111) single-crystal surface was prepared by cycles of Ar^+ sputtering followed by annealing at 900 K for 10 min. This procedure generates a clean and regular Au(111) surface as judged by Auger electron spectroscopy (AES) and STM. In each experiment metallic Mo ($10 \pm 2\%$ of a monolayer) is deposited onto the clean Au(111) surface kept at a temperature of 400 K in a sulfiding atmosphere (see below), and subsequently the sample is annealed at 723 K for 15 min while maintaining the sulfiding atmosphere. This procedure produces predominantly crystalline, single-layer MoS_2 nanoclusters as depicted in Figs. 1 and 2.

The atmosphere used for the sulfidation of Mo into MoS_2 is varied in terms of the partial pressures of H_2S and H_2. The synthesis gas is prepared by backfilling the vacuum chamber with hydrogen (H_2) and dihydrogensulfide (H_2S) to a total pressure of 2×10^{-6} mbar. Constraints imposed by the UHV equipment and the conditions of the experiment, however, limit the range of gas composition in terms of the P_{H_2S}/P_{H_2} ratio, since (i) a minimum H_2S partial pressure is required to fully sulfide the MoS_2 structures and (ii) the integrity of the UHV system limits the maximum achievable total pressure. Additionally, H_2S dosed from a lecture bottle (Praxair) has a nominal purity 99.8% with hydrogen being the major impurity. Therefore, two extreme cases were investigated in which the gaseous synthesis atmosphere consisted of either $H_2S{:}H_2 = 500$ (termed "sulfiding") or an excess of hydrogen gas $H_2S{:}H_2 = 0.07$ (termed "sulfo-reductive"). We emphasize that even at the lowest partial pressures of H_2S used in the experiments the majority of the clusters appear as fully crystalline MoS_2 nanoparticles (Fig. 2) with an interior structure similar to that of bulk MoS_2.

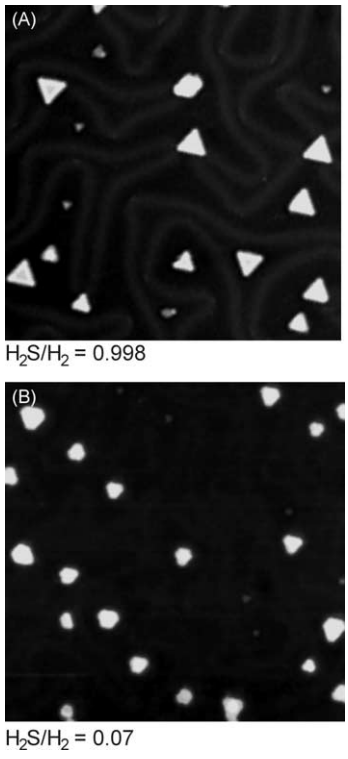

Fig. 1. Large-scale STM images showing the morphology of single-layer MoS_2 nanoclusters synthesized (A) in the fully sulfiding (723 K, $H_2S{:}H_2 = 500$), 408×413 Å^2, and (B) sulfo-reductive (723 K, $H_2S{:}H_2 = 0.07$) atmosphere, 450×460 Å^2. Under sulfiding conditions the predominant shape is the triangle. When the clusters are synthesized in excess hydrogen the predominant cluster shape is a truncated hexagon.

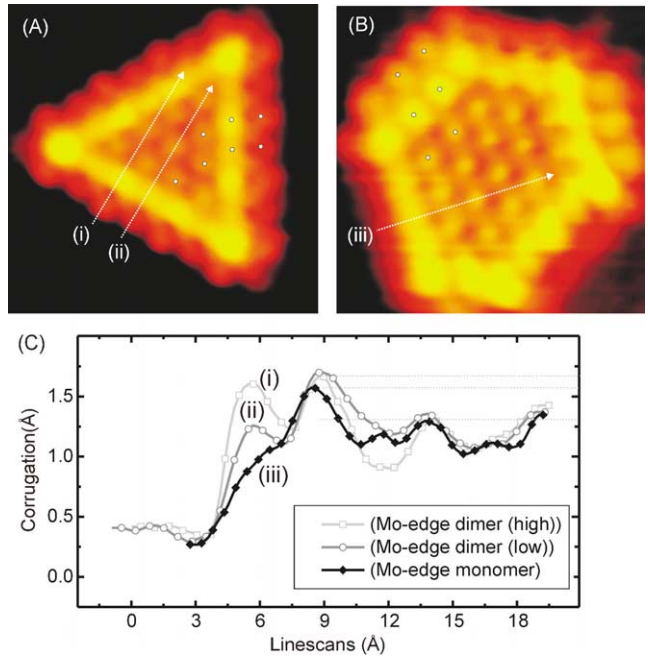

Fig. 2. (A) Atom-resolved STM image of a triangular single-layer MoS_2 nanocluster synthesized under the sulfiding conditions (45×46 Å^2, $V_t = -1250$ mV, $I_t = 0.86$ nA). (B) Atom-resolved STM image of a hexagonal single-layer MoS_2 nanocluster synthesized under the sulfo-reductive conditions (27×28 Å^2, $V_t = 39.1$ mV, $I_t = 0.31$ nA). White dots indicate the registry of protrusions at the edges. (C) STM corrugation measurements across the Mo edges of the triangle and hexagon. The scan orientations are indicated by white lines on both STM images. For the MoS_2 triangle two lines, (i) and (ii), are indicated since the fully saturated Mo edge exhibits a superstructure along the edge protrusions resulting in an alternating high/low pattern.

2.2. Density functional theory

The theoretical investigations are based on density-functional theoretical calculations, with a similar basic setup as reported in Ref. [31]. In order to realistically model the experimentally observed MoS_2 nanoclusters we have here carried out DFT calculations for a truncated, single-layer MoS_2 sheet positioned on a Au(111) substrate. The Au(111) surface is modeled by a rigid two-layer slab which is pseudomorphic with the MoS_2 lattice. When repeated in a supercell

geometry, an MoS_2 stripe terminated by two infinitely long edges results as depicted in Fig. 3B. The upper and lower edges are seen to be the so-called $(10\bar{1}0)$ Mo edge and $(\bar{1}010)$ S edge, respectively.

The density-functional calculations are then carried out as follows [42]: the Kohn–Sham (KS) wave functions and the electron density are expanded in plane waves with kinetic energies below 20 and 25 Ry, respectively [43]. The first Brillouin zone is sampled by a discrete one-dimensional grid consisting of 12 k points, and ultrasoft pseudopotentials [44] are used to model the ionic cores. The PW91 functional [45] is used to model exchange and correlation effects. The calculational scheme proceeds by diagonalizing the KS Hamiltonian iteratively and the resulting eigenstates are populated according to the Fermi distribution. The Pulay mixing of electron densities is applied, and the whole procedure is repeated until a self-consistent density is obtained. In all calculations the MoS_2 stripe is allowed to relax according to the calculated Hellmann–Feyman forces.

From the DFT results, simulated STM images of the MoS_2 edges are calculated on the basis of the Tersoff–Hamann formalism [46] where the tunneling matrix elements are evaluated using the self-consistent KS wave functions. The contour value used for generating the STM images of the edges is chosen so that the calculated corrugation of bulk MoS_2/Au(111) becomes equal to the measured corrugation in the interior of the MoS_2 nanoclusters. The experimentally measured corrugation on the basal plane of 0.22 ± 0.05 Å was reproduced with contour values corresponding to an LDOS of $\rho(r_0, E_F) = 8.3 \times 10^{-6}$ electrons/(eV · Å^3).

3. Results and discussion

In the vast HDS literature the active sites for HDS have generally been believed to be localized at the edges of the MoS_2 clusters. A detailed description of the activity of hydrotreating catalysts has, however, been missing due to the lack of direct atomic-scale insight into the structures existing at the cluster edges. In this respect, a direct characterization of the actual morphology of the MoS_2 clusters is of utmost importance, since the possible edges terminating the clusters are structurally and electronically dissimilar and are therefore expected to possess very different catalytic properties. The present STM experiments directly provide information on this important issue for the gold-supported MoS_2 nanoclusters.

Atomically resolved images of two MoS_2 nanoclusters produced by the procedures discussed in the experimental section are displayed in Figs. 2A and B, for the sulfiding and sulfo-reductive conditions, respectively. Both of the clusters display a flat basal plane with protrusions arranged in a hexagonal pattern and an interatomic distance of 3.15 ± 0.1 Å. This is in exact agreement with the interatomic distances on the (0001) basal plane structure of MoS_2. In the bulk form, MoS_2 is a layered material with each layer consisting of S–Mo–S trilayers held together by weak van der Waals forces. Within a single layer (see Fig. 3) the Mo atoms are arranged in a hexagonal lattice and positioned with a trigonal prismatic coordination to six S atoms. From the average apparent height of 2.1 Å in the STM images, it is concluded that all the clusters under investigation are single-layer MoS_2 slabs oriented with the (0001) facet in parallel with the Au(111) substrate.

3.1. Morphology

For both the synthesis of MoS_2 nanoclusters in a sulfiding or sulfo-reductive atmosphere, the STM experiments (Fig. 1) show that the clusters have an average size of about 600 ± 200 Å^2. This corresponds to 30 to 50 Mo atoms per cluster, which is a size often encountered in industrial HDS catalysts [7] and from this perspective, the present model system is therefore suitable for obtaining further relevant insight. The exact composition of the gaseous atmospheres used for the synthesis of the MoS_2 nanoclusters is, however, observed to have a profound impact on the actual cluster morphology. This is clearly revealed by the large-scale STM images (Fig. 1) obtained for the experiments in the sulfiding and sulfo-reductive environments, respectively. When synthesized under the most sulfiding conditions (H_2S:$H_2 = 500$), Fig. 1A, the STM images reveal that the MoS_2 clusters adopt a *triangular shape*. This is in accordance with the findings in our previous study [20], and suggests that the triangular shape is the equilibrium form of MoS_2 nanoclusters under highly sulfiding conditions. When more reducing (H_2S:$H_2 = 0.07$) conditions are used for the synthesis (Fig. 1B), the triangular MoS_2 clusters, however, cease to dominate. Instead we observe the emergence of another type of MoS_2 structure with a *hexagonal morphology*. Hence, it appears that the equilibrium shape of MoS_2 clusters is sensitive to the different gas compositions used in our experiment. The present results are the first direct atomic-scale observations of such changes in the MoS_2 morphology.

The STM experiments (Figs. 1 and 2) also show that the morphology changes caused by the different sulfiding procedures do not result in large variations in the absolute number of edge sites (i.e., the edge dispersion remains quite constant). Nonetheless, a dramatic change in the type of edges exposed is found. In fact, one of the edges exposed in the truncated hexagons obtained after the more reducing sulfur-reductive synthesis conditions is completely absent in the MoS_2 nanoclusters synthesized in the more sulfiding environment. Such structural differences are likely to influence the catalytic activities/selectivities profoundly and in order to obtain further insight into the nature of the different structures, the atomic-scale structure will be discussed below in terms of the new insight provided by STM.

Single-layer MoS_2(0001) clusters are in their equilibrium shape expected to be truncated by either (or both) of two possible low-indexed (low Gibbs energy) edge terminations, the $(10\bar{1}0)$ Mo edge and the $(\bar{1}010)$ S edge. In Fig. 3 the struc-

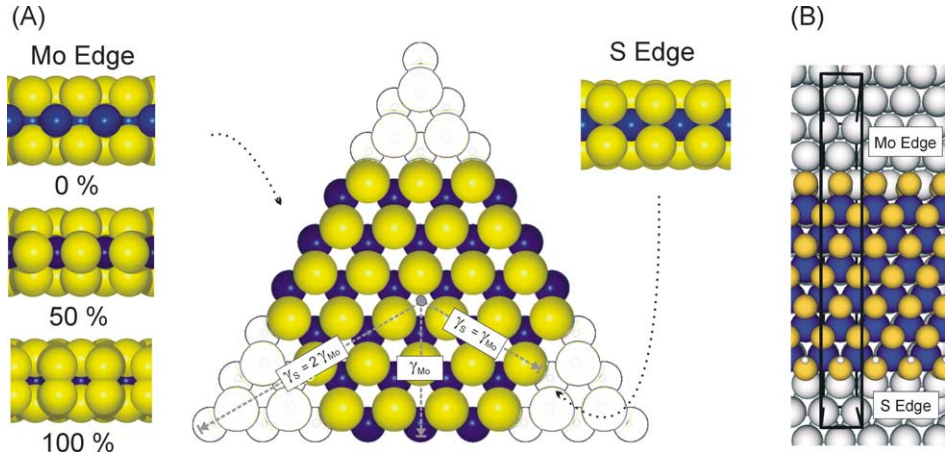

Fig. 3. (A) Atomic ball model (top view) showing a hypothetical, bulk-truncated MoS_2 hexagon exposing the two types of low-index edges, the S edges and Mo edges. The Mo atoms (blue) at the Mo edge are coordinated to only four S atoms (yellow). To the left the stripped Mo edge is shown in side view together with two more stable configurations with S adsorbed in positions predicted from theory; the 50% covered (monomer) and a 100% covered Mo edge (dimer). Right is shown a side view of the S edge with a full coordination of six sulfurs per Mo atom. Plotted on the MoS_2 hexagons are vectors with lengths corresponding to the edge free energies γ_{Mo} for the $(10\bar{1}0)$ Mo edge and γ_S for the $(\bar{1}010)$ S edge. The envelope of tangent lines drawn at the end of each such vector constructs a hexagon if γ_S equals γ_{Mo}. If $\gamma_S > 2 \times \gamma_{Mo}$ the result is a triangle (outlined shape) terminated exclusively by the Mo edge, or vice versa for the S edge. Intermediate values result in clusters with a hexagonal symmetry. (B) The setup used for the DFT calculations, showing the $MoS_2(0001)$ stripe (top view) supported on a two-layer thick epitaxial Au(111) substrate. Au atoms are indicated with large grayish balls. The MoS_2 stripe is terminated by the Mo edge (upper) and the S edge (lower). Within a single unit cell the stripe consists of a single row of Mo atoms parallel to the edge and six rows of Mo atoms perpendicular to the edge.

ture of both these edges is illustrated in a ball model of a hypothetical, hexagonal MoS_2 nanocluster obtained by truncating an infinite sheet of $MoS_2(0001)$. In an equilibrium situation, the actual shape of the MoS_2 clusters is directly determined by the relative stability of these two types of edges. For instance, predominantly triangular MoS_2 clusters with all three sides truncated by the same type of edge imply that the exposed edge type is considerably more stable than the other. Hexagonal-like clusters, on the other hand, will be terminated by both types of edges and imply that the two edges have a comparable stability. The dispersion of the two types of edges in the clusters can be quantified in more detail in terms of a simple Wulff construction [47,48], which expresses the equilibrium shape of a cluster as a function of the ratio of edge free energies (Fig. 3). The observed triangular morphology under sulfiding conditions (Fig. 1A) implies that the ratio of the edge free energy of the S edge to Mo edge (γ_S/γ_{Mo}) is greater than two or less than a half, depending on which edge termination is the more stable one. Under the more reducing (sulfo-reductive) conditions, however, the observed hexagonally truncated morphology (Fig. 1B) implies that the ratio of (γ_S/γ_{Mo}) lies in the range 0.5 to 2. As will be concluded below, the Mo edge dominates for all the observed clusters and the ratio is therefore restricted to the interval $1 < \gamma_S/\gamma_{Mo} < 2$ under the conditions of the sulfo-reductive experiment.

3.2. Edge structures

The determination of which type of edges that terminate the MoS_2 nanoclusters is not straightforward since, as pointed out in several DFT studies [26,28,29,32], the actual edge structures may be quite different from the Mo and S edges expected from simple terminations of the stoichiometric bulk MoS_2 structure. A further complication is related to the fact that both Mo and S edges may undergo structural transformations depending on the conditions and exist in different structural modifications (see, e.g., Fig. 3). In order to address this issue, at least three factors must be taken into account: (i) the sulfur coverage at the edges, (ii) coverage with H adsorbates, and (iii) structural reconstructions relative to bulk MoS_2 due to the changed coordination of the edge atoms.

Several different edge terminations are possible, even if we consider the sulfur coverage only. The hypothetical, bare Mo edge shown in Fig. 3 is terminated by a row of undercoordinated Mo metal ions (coordinated to only four S atoms). Previous studies have shown that this situation is very unfavorable and that such edges will have a high affinity toward S adsorption. The S will adsorb preferentially in two almost equally stable configurations [26,28,32,49], where one S atom (50% S coverage) or two S atoms (100%) coordinate to each Mo edge atom. In both cases every Mo atom achieves a sixfold coordination to sulfur. In a 50% coverage situation the S atoms will, however, as illustrated by the ball model in Fig. 3, not occupy normal lattice sites. Rather a significant reconstruction takes place: the S monomers are seen to be shifted by half a lattice constant relative to the bulk S lattice, and they move down to a bridging position in-plane with the Mo lattice. For the fully covered Mo edge (100%) the sulfur atoms laterally coincide with the bulk S lattice, but they display a small pairing perpendicular to the $MoS_2(0001)$ surface, thus forming S_2 dimers or disulfide-like species. For the second edge type (the S edge in Fig. 3),

the maximum coordination to six sulfur atoms is achieved in one stable configuration where the edge is terminated by a row of sulfur atoms positioned in bridge positions close to those expected from bulk-terminated MoS_2.

In order to determine the nature of the edges which are exposed under the different experimental conditions, high-resolution STM images are recorded (Figs. 2A and 2B) and these will be discussed in the following sections. Before doing so, it is, however, important to emphasize that STM images generally reflect a rather complicated convolution of the geometric and the electronic structure of the surface, and not only simple geometric information. According to the Tersoff–Hamann theory [46], low-bias STM images in the constant-current mode reflect, to a first-order approximation, contours of constant local density of electronic states (LDOS) at the Fermi level of the surface structure projected onto the position of the tip apex. In this respect, the electronic structure of the MoS_2 clusters is very interesting, since bulk MoS_2, consisting of infinite sheets of S–Mo–S, is semiconducting and displays a bandgap of ≈ 1.2 eV [50,51]. The absence of electronic states at the Fermi level available for tunneling in bulk MoS_2 thus implies that the clusters should be impossible to image at bias voltages numerically lower than half the value of the bandgap. This is clearly not the case, and it is found that STM images of the MoS_2 clusters are possible at any tunneling bias on both sides of the Fermi level. This means that the electronic structure of the clusters must be perturbed relative to bulk MoS_2, and in the next sections we show that the MoS_2 nanocluster edges in fact become entirely metallic and demonstrate how this can be used to identify the types of edges observed with STM.

3.2.1. *MoS_2 triangles*

In the case of clusters synthesized in a fully sulfiding atmosphere (Fig. 2A), the structure of the edges is identical to that observed in a previous study of triangular MoS_2 nanoclusters [20]. The predominant triangular shape immediately implies that only *one* of the two feasible edge types is exposed, the Mo edge *or* the S edge. In the STM images of the triangular MoS_2 clusters, the edges appear perturbed relative to the basal plane with two pronounced signatures: (i) a striking bright brim ~ 0.3 Å above the basal plane extending around the cluster perimeter and (ii) an apparent shift of half a lattice constant of the outermost protrusions compared to the basal plane protrusions. In Ref. [37] it was shown that these two signatures are the result of a significantly perturbed electronic structure at the edges terminating the basal plane of the MoS_2 nanocluster. In fact, two edge-localized electronic states are found to cross the Fermi level in the DFT-derived electronic band structure of the fully sulfur-saturated Mo edge (100% S), thereby rendering the edges metallic in contrast to the semiconducting basal plane. Fig. 4 shows a simulated STM image of the Mo edge fully saturated with S_2 dimers (100%) and supported on a Au(111) substrate. The simulation of this edge type is seen to reproduce all of the prominent features along the cluster edges

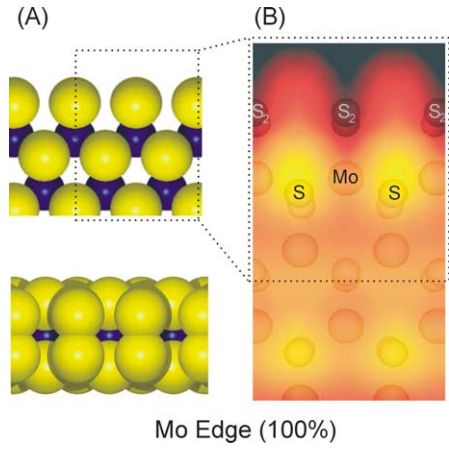

Fig. 4. (A) Ball models of the Mo edge with S_2 dimers (100% S) in top and side view. (B) A simulated STM image of a two-atom wide part of the Mo edge (100% S). For clarity the Au atoms are omitted in the graphical representation.

in the STM image. It is interesting that the edge protrusions in the STM image are found not to coincide with the positions of the S_2 dimers, but rather to reflect the interstitial region between neighboring S_2 dimers. The bright brim, which is also associated with a metallic edge state, is furthermore fully reproduced in the simulation and is located in the row adjacent to the edge protrusions. Hence, it is concluded that triangular MoS_2 clusters are terminated by Mo edges fully covered with S_2 dimers [20,37] and that these edges are metallic [52].

One may not anticipate such fully sulfided MoS_2 structures to be very reactive, since it is generally believed that sulfur anion vacancies or coordinatively unsaturated sites located near the edge must be created in order for the cluster to be active in hydrodesulfurization. Although such vacancy sites may be important in HDS, it is interesting that a recent STM study found that the metallic edge states associated with the brim on the fully sulfided MoS_2 triangles contain unusual sites that are involved in adsorption and reactions of reactants [22]. As will be evident below, similar electronic states are observed in the present study to exist on several other types of MoS_2 edge structures, which suggests that such unusual metallic sites may also play a more general catalytic role, also for the MoS_2 hexagons.

3.2.2. *MoS_2 hexagons*

An atom-resolved STM image of a typical hexagonally truncated MoS_2 nanocluster synthesized under sulfo-reductive conditions is shown in Fig. 2B. The hexagonal shape immediately implies that both S edges and Mo edges terminate the clusters in this case. In view of this, a detailed analysis interestingly reveals that neither of the two types of edges in the hexagonal single-layer MoS_2 structures displays the characteristics of the fully S_2 dimer-covered Mo edges found in the MoS_2 triangles. In addition to the large change in morphology, the detailed structure of the Mo edges has thus changed under the more reducing conditions. As dis-

cussed in Section 3.1, the presence of truncated hexagons indicates that the free energy Mo and S edges now are comparable. In the MoS_2 hexagons, both of the new edges appear electronically perturbed relative to the bulk and the STM images reveal "brims" near the edge with high electron state densities, which suggest that metallic one-dimensional edge states exist on these edges. One of the two edge types is furthermore observed to be characterized by a very low intensity at the outermost row. For this edge type, the height of the brim above the basal plane is found to be 0.25 ± 0.10 Å, i.e., a little smaller than the brim for the Mo edge with S_2 dimers in the MoS_2 triangles which is 0.30 ± 0.10 Å. In Fig. 2C, the graph shows an STM line scan perpendicular to this type of edge in the hexagon-shaped cluster and the equivalent scans for a triangular cluster terminated with S_2 dimers on the Mo edge. The line scan for the former shows that the STM contrast near the edge falls off rapidly as the brim is crossed. This lack of corrugation in the STM images implies that the LDOS at the Fermi level at these edges is vanishingly small.

To identify the origin of the experimentally observed edge structure, we have performed DFT calculations and used the calculated electron densities to simulate STM images of the MoS_2 edges. In these calculations, edges with a lower coverage of sulfur than the fully saturated dimer-covered edges have also been considered, since they may be favored in the absence of a high chemical potential of sulfur during synthesis. In particular, Mo edges with monomers (50% S) have been considered since such structures are quite stable (Fig. 3) [25,26,28,49]. In Fig. 5B a simulated STM image of this edge is shown. The S monomer configuration is seen to fully reproduces the details of the one type of edge described above for the MoS_2 hexagons. Interestingly, the outermost S atoms are not imaged at all; i.e., the LDOS at the Fermi level is zero here [53]. The simulated image also reproduces the bright brim extending along the row behind the S monomers, and we thus propose that the Mo edges of the MoS_2 hexagons synthesized under the reducing conditions of the experiment are terminated by S monomers. In addition to the changed morphology imposed by the change in synthesis conditions, the results thus show that the stability between the monomer and the dimer coverage on the Mo edge has shifted in favor of the monomers as more reducing conditions are introduced in the experiment. Later we will investigate this transition in further detail.

The other, more intense edges of the MoS_2 hexagon in Fig. 2B are from the symmetry of the MoS_2 crystal structure associated with S edges. Here, the protrusions at the edges are clearly imaged, and by superimposing a grid on the basal plane S atoms, the edge protrusions are observed to be *in* registry with the sulfur atoms on the basal plane. The STM images also reveal a rather intense brim adjacent to the outermost row of protrusions on the S edges, which indicates the presence of metallic one-dimensional states, also on this type of edge. The corrugation of this brim above the basal plane is found to be 0.50 ± 0.10 Å. This is significantly higher than the corresponding value for the corrugation on the S monomer-covered Mo edges on the hexagons (see above) or on the dimer-covered Mo edges found in the MoS_2 triangles. Unlike the brim on the Mo edge where the corrugation is very low in the direction along the edge, the corrugation along the S edge brim is pronounced with protrusions emerging with the characteristic 3.15 Å periodicity of MoS_2. If we tentatively assume that the brim and edge protrusions reflect the position of S atoms at the S edge, the in-registry position then suggests that the S edges adopt a structure very similar to the simple continuation of the bulk MoS_2 lattice (see Fig. 3). Recent STM simulations of such simple S edge terminations are, however, not in accordance with the experiments, since they display a periodic superstructure along the edge [31] or a brim that extends all the way to the cluster edge [30]. Alternatively, one could expect structures with a reduced coverage of S to form under the reducing conditions, but these structures would break the symmetry of the lattice, and since we find, without exceptions, a periodicity of one lattice constant along the S edge (up to 9 atoms wide was observed), edge structures with a reduced S coverage therefore cannot account for the experimental observations.

If instead we include in the model the possibility of hydrogen atoms being adsorbed on the S edges other more stable structures will result, which can account for the experimental observations. Indeed, a fully covered S edge with hydrogen atoms adsorbed is found to match the STM images closely, and this configuration also turns out to be energetically very stable. A large number of possible adsorption sites for H on the S edge have recently been investigated, and in contrast to the Mo edge, H is found to bind strongly to the S edge [31,34,36]. A ball model of the most favorable adsorption site is illustrated in Fig. 5D. The hydrogen atoms are seen to adsorb on one side of the S edge atoms in a position slightly behind the outermost sulfur row, pointing toward the basal plane. The associated hydrogen-binding energy at zero temperature is rather large, $\Delta E_{\mathrm{H}} \simeq -1.26\ \mathrm{eV}/\mathrm{H}_2$ molecule. The presence of hydrogen is seen to result in an upper S–H group and a lower S atom, see Fig. 5D. A simulated STM image of this configuration can be seen in Fig. 5C, and indeed all the experimentally observed features are reproduced: (i) the outermost protrusions are associated primarily with the S–H groups, and (ii) in the row behind, a pronounced bright brim is also seen. Several other slightly less stable configurations exist for hydrogen on the S edge [31, 34,36], and a random distribution of H between these could in principle be possible at higher temperatures. At room temperature, we can, however, rule this out since a random distribution would most certainly be visible in the STM images by periodicities of edge protrusion larger than one, which is the only periodicity we observe. Hence, we conclude that the S edges terminating the hexagonal MoS_2 nanoclusters are fully covered with S and adsorbed hydrogen species.

These results represent the first direct evidence of the location of S–H groups at the MoS_2 edges. Previous spectros-

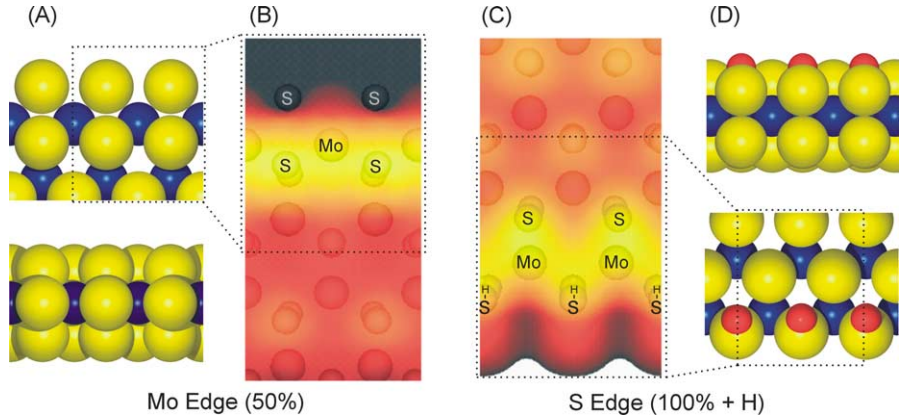

Fig. 5. (A) Ball model (top and side view) of the Mo edge with monomers (50% S). (B) A simulated STM image of the Mo edge S monomers (50%). (C) A simulated STM image of the S edge (100%) with hydrogen adsorbed. (D) A corresponding ball model (top and side view) of the S edge with hydrogen (red) adsorbed on the upper S atoms. For both simulated images the contour value is $8.3 \times 10^{-6}(\mathrm{eV\,\AA^3})^{-1}$ and the color scale corresponds to a corrugation of 1.5 Å. For clarity, the Au substrate is omitted in the graphical representations.

copy-based measurements [13] have indicated that S–H groups are present at the edges of the MoS_2 phase, but these studies have given little direct insight into the exact location and coordination of such species. Given the fact that H adsorbs strongly on the S edge of MoS_2 under the conditions of our experiment (Fig. 5D), we suggest that the previously observed S–H groups are identical to these. This insight is important since hydrogen species preadsorbed on the cluster edges are believed to play a central role in the catalytic reactions, i.e., in the hydrogenation and hydrogenolysis of the sulfur containing molecules in the oil feed. A detailed analysis [31] of the electronic band structure reveals that the S edge configuration with hydrogen adsorbed (Fig. 5D) indeed has a single, localized metallic edge state, which gives rise to the characteristic bright brim near the cluster edge in the STM image. In view of recent STM experiments and DFT calculations [22], where the one-dimensional metallic edge states on the fully sulfided Mo edges of the MoS_2 triangles were found to contain favorable adsorption and reaction sites for S-bearing molecules, it is suggested that the similar metallic brims on the S edges of the MoS_2 hexagons may also play an important role in the catalysis. It is likely that the close vicinity of coadsorbed H atoms on the edges may then facilitate an immediate hydrogenation reaction. Since the hydrogen atoms furthermore adsorb more readily on the S edges than on the Mo edges, this may favor such reactions. Additional experiments with probe molecules like thiophene are planned in order to investigate this.

In summary, we conclude that the single-layer MoS_2 nanoclusters synthesized under the sulfo-reductive conditions of our experiment adopt a hexagonally truncated shape, terminated by Mo edges with S monomers (50%) and hydrogen-covered, fully sulfur-saturated S edges. In the next section the thermodynamic stability of the different structures will be investigated and the results will be extrapolated to real process conditions involving high pressures and temperatures.

3.3. Thermodynamic stability of the MoS_2 edges

In the STM experiments presented above it was demonstrated how the relative stability of the two types of MoS_2 edges changes as a function of the gas-phase composition resulting in a change in the cluster shape. These results are very interesting from a catalysis point of view since they will allow one for the first time to base HDS models on direct atomic-resolved insights into the structural properties of the catalytically relevant MoS_2 nanoclusters. Previous observations have only in a qualitative way allowed one to conclude that the activity resides at the edge regions of MoS_2 (see, for example [11,12,54–57]). An important conclusion from the STM findings is that dynamical structural and morphological changes appear to be essential to include into the description of the catalysis. Under catalytic process conditions, it is likely that single S atoms are removed from the edges by reaction with hydrogen, thus leading to the formation of so-called sulfur vacancies or coordinatively unsaturated sites, which is believed to be an important step in HDS. A mapping of phase diagrams for the thermodynamically most stable edge structures is therefore of high interest to study the reaction energies involved in the formation of vacancies on these edges. Under the sulfo-reductive conditions of the MoS_2 synthesis we find experimentally that the S coverage on the Mo edges has already decreased (Fig. 5D) relative to a 100% S coverage. In contrast, the S edges are not observed to have a lower sulfur coverage under the conditions of our experiment. Instead, the response of the S edges to a higher partial pressure of H_2 during synthesis is to adsorb H species on the fully saturated edge (Fig. 5D). In the following, we will relate the STM experiments to the theoretically predicted stabilities of the different edge configurations established by use of a thermodynamic model, where the zero-temperature, zero-pressure DFT energies are extended to the finite pressures and temperature of the experiments by consideration of the chemical potential of reaction gasses.

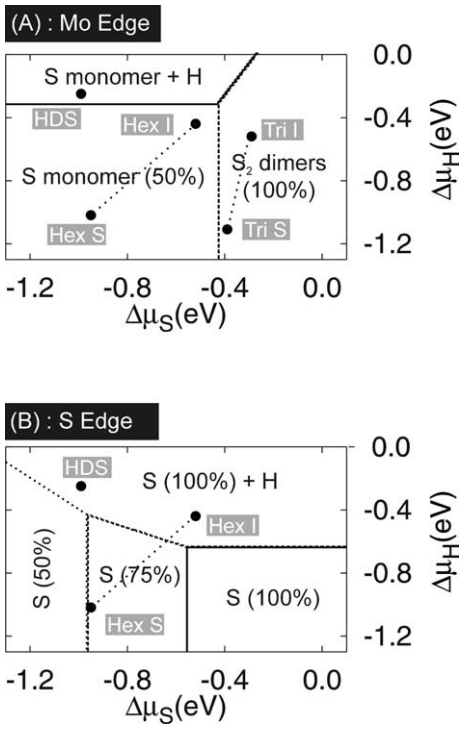

Fig. 6. Phase diagrams for (A) the Mo edge and (B) the S edge with regions indicating the stable configurations for realistic values of $\Delta\mu_S$ and $\Delta\mu_H$. For the Mo edge the presence of Au is taken into account. The chemical potentials have been normalized with respect to the energy of bulk sulfur and half the energy of a single, isolated H_2 molecule. The labels refer to the experimental conditions (see text) and typical HDS conditions.

We use a general methodology that has previously been applied in Refs. [28,30,32,58,59]. Further details on the specific thermodynamic scheme are given in Ref. [31], where similar calculations are presented for the MoS_2 edges without the influence of the gold substrate. In Fig. 6 the phase diagrams constructed from the DFT energies are directly displaying the expected stability regions for adsorbates on the S edges and Mo edges as a function of the chemical potentials of sulfur and hydrogen.

The synthesis parameters used for the experiments in this paper represent single points corresponding to specific values of μ_S and μ_H in the phase space of possible edge structures of MoS_2, and we can therefore compare directly the predicted and observed edge stoichiometries in Figs. 6A and B, respectively. The chemical potentials of S and H are calculated from standard thermodynamic tables [60] by the partial pressures of H_2S and H_2 and the given temperature of the sample. Due to the "quench-and-look" nature of the experiments it is, however, necessary to consider a range of parameters in this phase space, instead of just one point for each experiment. The synthesis and subsequent STM imaging were done under different conditions, and it is not a priori clear to which extent the edge stoichiometry changes as the conditions are gradually shifted from synthesis to imaging conditions. If there is a change of stability when imaging conditions are approached, one of two extreme situations should be considered: Either some degrees of freedom are frozen out and the clusters are imaged as in the synthesized state, or the reaction kinetics favor a phase transition, and in this case the edge structure is determined by the imaging conditions. This could, for example, happen through desorption/adsorption processes as the sample cools and the low base pressure of the vacuum system is achieved. Since neither of these possibilities can immediately be ruled out, both the extreme points corresponding to imaging and sulfidation will be indicated in the following analysis. It is assumed that the kinetic barriers for substantial morphology changes are too large for it to take place as we cool the sample and remove the synthesis gas. We therefore expect that the observed morphologies closely reflect those existing under synthesis conditions, and that the change to imaging conditions has only a potential effect on the detailed edge structure. The chemical potentials under synthesis conditions were estimated from the values quoted in the experimental section. At the other extreme during STM imaging, μ_S and μ_H were estimated at 300 K and with (low) partial pressures (3×10^{-10} mbar range) of H_2S and H_2 registered from the background composition after the synthesis. We note that the rest gas composition under imaging conditions typically differed between the two types of experiments.

3.3.1. Thermodynamic stability of the Mo edges

Fig. 6A shows the phase diagram indicating the stable structures at the Mo edges for different values of μ_H and μ_S. It is seen that three different edge configurations may be stable depending on the thermodynamic conditions. Focusing first on low values of μ_H, either S monomers (50% S) or S_2 dimers (100% S) are expected to be present at the Mo edge, and there is a transition between the two configurations at $\Delta\mu_S \sim -0.43$ eV. For high values of μ_H another structure is stable which involves coadsorption of hydrogen [31]. In this regime hydrogen is expected to be present at the Mo edge forming an S–H group with every second S monomer [61].

For the STM experiments performed under sulfiding conditions, the values of the chemical potentials under both synthesis (S) and subsequent UHV imaging (I) corresponding to the MoS_2 triangles (Fig. 2A) are indicated in Fig. 6A by the points labeled Tri S and Tri I, respectively. In both situations the S_2 dimer configuration is expected to be the preferred structure, which is in excellent agreement with the STM analysis. Under the synthesis conditions (Tri S) the chemical potential, however, comes close to the transition line (due mainly to the higher temperature) and in fact if we omit the influence of the Au substrate and calculate it for a unsupported MoS_2 slab, the stability is shifted and the monomers now become stable even under sulfiding conditions.

By increasing the partial pressure of H_2 during synthesis going to the sulfo-reductive conditions, the main response is a reduction of the chemical potential of sulfur μ_S. The point (Hex S) shown in the phase diagram corresponds to the reducing conditions during synthesis of the MoS_2 hexagons. It is seen to be positioned well inside the region where the

monomers are stable. Under the imaging conditions (Hex I), the phase diagram shows that the chemical potential of sulfur moves closer to the transition line between dimers and monomers, but does not cross it. Hence, the imaging and sulfidation environments are not expected to be separated by a structural transition, and these findings are in good agreement with the analysis of the experimental STM image in Fig. 2, where we observe the sulfur monomers to be the stable edge structure.

To conclude, the thermodynamic model presented here predicts correctly how the Mo edges of the single-layer MoS_2 nanoclusters adopt either a fully saturated S_2 dimer coverage or a half-saturated S monomer as a function of the conditions under which the cluster is synthesized. In Fig. 3 the geometric structure of both edges is shown, and it is seen that any transition between them must be associated with a rather large geometrical reconstruction. Whereas the S_2 dimers are *in* registry with the positions of the basal plane S atoms, the S monomers are located *out* of registry and have moved down into the plane of Mo atoms. We therefore expect that the transition between the two is associated with a significant activation barrier. Evidence of such a barrier associated with the edge restructuring is provided by further experiments, where the hexagonally shaped MoS_2 clusters are resulfided with H_2S and imaged with the STM. Simply exposing the clusters to gaseous H_2S corresponding to a background pressure of 2×10^{-6} mbar did not result in the formation of dimers, despite the fact that dimers should be favored at the large chemical potential of S ($\Delta\mu_S > -0.4$ in Fig. 6A) corresponding to sulfiding conditions. Only by activating the process by heating above 573 K could the S_2 dimers be formed on the Mo edges of the hexagonal MoS_2 clusters, indicating that a substantial energy barrier is associated with the structural transition from monomers to dimers. An example of a resulfided hexagonally shaped cluster is depicted in the STM image in Fig. 7, where the signatures of the Mo edge with dimers are evident on the longer edges, i.e., clearly visible edge protrusions imaged out of registry and a bright brim. Since this only occurs above 573 K, we conclude that the transition between monomers and dimers is an activated process, meaning that the opposite process (i.e., vacancy formation from the dimers) is activated as well. This is in agreement with previous STM results, where large exposures of highly reactive atomic hydrogen to the fully saturated Mo edges led to the formation of only a few vacancies [20].

Furthermore, we note that large-scale STM images from the resulfidation experiments showed that the overall morphology does not immediately transform back to the triangular shape which is very predominant when the MoS_2 nanoclusters are synthesized directly under the more sulfiding environment (Fig. 2A). Likewise, when the triangular MoS_2 nanoclusters (Fig. 2A) are exposed to large dosages of atomic or molecular hydrogen at high temperatures (see, for example, [20]), the STM images did not show any substantial tendency for shape transformation either. This indicates

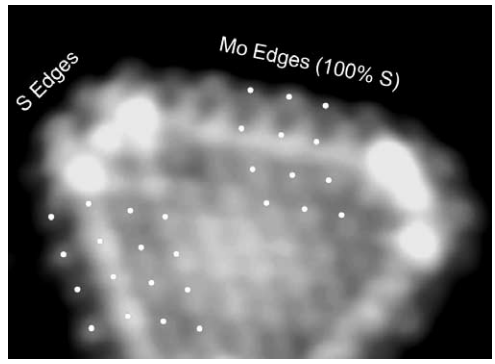

Fig. 7. An atom-resolved STM image of a typical single-layer MoS_2 hexagon exposed to H_2S gas at 573 K. The white dots indicate the registry at the longer (Mo) edges. The registry of edge protrusions and the bright brim reveals that the Mo edges have become resulfided to the fully saturated S_2 dimer configuration (compare with Fig. 2A).

that large activations barriers are associated with such dynamic transformation processes, and this is very interesting in relation to previous measurements of catalytic activity that have shown large irreversibilities depending on the sulfiding conditions [24]. We will treat this issue in detail in a forthcoming paper [62].

When the chemical potentials are calculated with typical values found during HDS conditions (in terms of $T = 650$ K, $P_{H_2} \simeq 10$ bar, and $P_{H_2S} \simeq 0.1$ bar) one can estimate from the phase diagram which edge structures are expected to be stable. This is shown by the point indicated by HDS in Fig. 6A. It is found that the S coverage is expected to be the same as for the MoS_2 hexagons, i.e., S monomers. The higher chemical potential of H, however, means that stable S–H groups will begin to form at the S monomers.

3.3.2. Thermodynamic stability of the S edges

In Fig. 6B the corresponding phase diagram for the S edges is shown, indicating the predicted edge configurations in terms of the S and H coverage. Again points with values of μ_S and μ_H are plotted referring to the synthesis parameters used for the sulfo-reductive conditions (Hex S) and typical conditions for STM imaging (Hex I). In agreement with the STM analysis, the thermodynamic model correctly predicts that the fully S covered edge with hydrogen adsorbed is expected to be stable under imaging conditions (Hex I). The diagram, however, predicts that a different structure, a reduced S edge (from 50 to 75%), is stable during synthesis (Hex S), and, hence, that the two points are separated by a phase transition. The fact that fully sulfided S edges (with H coadsorbed) is the only type observed with STM implies that this transition from the defected 50–75% covered S edge to a fully sulfided S edge is not hindered by kinetic effects. This may be explained by the less severe geometrical restructuring associated with the transitions, which basically only involves S adsorption (e.g., from H_2S in the rest gas) on a vacancy site on the reduced edge. The present diagram does not include the presence of an Au surface, and it can at present not be entirely ruled out that the substrate gives

rise to changes in the energetics of the S edge, as described above for the Mo. Preliminary results, however, suggest that the changes due to Au are small and that they do not change the qualitative conclusions concerning the stability of the S edge.

The large energy associated with hydrogen adsorption ($\Delta E_H \simeq -1.26$ eV/H_2 molecule) means that hydrogen atoms will saturate the S edge at a rather low chemical potential, and the thermodynamic model also predicts that the isolated S edge has hydrogen adsorbed, in full accordance with the experimental observations; see Fig. 5D. Interestingly, this configuration is also the one that is predicted to be stable under reaction conditions (see point HDS in Fig. 6B), and this supports our conclusion that the observed S–H groups are identical to the species believed to be present during HDS.

The increased stability gained by adsorbing hydrogen at the S edges is also important in relation to the formation of sulfur vacancies. In STM experiments, no indications were seen that vacancies could be formed on the S edge, even by rather large exposures of atomic hydrogen (10^{-6} mbar H_2 gas dissociated on a glowing W filament [63]). Hence, it is concluded that the selectivity of the S edge with respect to formation of vacancies or S–H groups is in favor of the latter under the conditions of the experiment. This is also clear from the phase diagram since the starting point in the experiment is the stable S edge with S–H groups. Dosing atomic hydrogen only increases μ_H and will merely tend to stabilize the hydrogen already adsorbed on the fully covered S edge even further.

4. Conclusions

In conclusion, atom-resolved STM images of gold-supported MoS_2 clusters are used to obtain new morphological and structural insight into the type of MoS_2 structures present after different synthesis conditions relevant to sulfidation and operation of HDS catalysts. The present results show that the morphology of MoS_2 nanoclusters in the catalyst may in fact be very complex, since the MoS_2 clusters do not seem to have a fixed shape. Rather, the clusters adopt their shape according to the conditions under which they are synthesized, e.g., triangles under heavy sulfiding conditions (catalyst activation) or truncated hexagons under more sulfo-reductive conditions resembling HDS conditions. These results are remarkable since in the absence of direct insight most past models have assumed a hexagonal MoS_2 morphology irrespective of the type of conditions that were used. The observed morphology changes are, however, expected to have a strong impact on the catalysis. In fact, it is found on the basis of atom-resolved STM images and image simulations that truncated hexagons have an edge termination (the S edge), which is completely absent in the triangular MoS_2 structures. This means that large changes in both the absolute and relative concentration of different types of edge sites (sulfur monomers, dimers, S–H groups, vacancies, metallic brim sites, etc.) exist. Such differences are expected to have a profound influence on catalyst activities and selectivities.

The detailed atomic-scale structure of the catalytically important edges in MoS_2 was solved by combining the experimental STM images and simulations from theoretical DFT calculations, which included the effect of hydrogen adsorption on the edges and the potential influence of the gold model substrate. Whereas the triangular MoS_2 nanoclusters synthesized under sulfiding conditions were found to be terminated by fully saturated Mo edges, the hexagonal clusters are exposing two different types of edges, Mo edges covered with S monomers and fully sulfur-saturated S edges with H atoms adsorbed (i.e., S–H groups). This means that we have obtained the first direct evidence for the exact location of S–H groups, which are believed to be important in HDS as a source of hydrogen atoms. For all the types of MoS_2 edges observed in the present experiments, it is found that the electronic structure is dominated by metallic one-dimensional edge states. In view of recent studies, it is speculated that these may play an important role in the catalysis [22]. In these studies performed on the triangular MoS_2 nanoclusters, it was surprisingly observed that the fully sulfided Mo edges (i.e., Mo edges containing no CUS sites) are quite reactive. The activity could be associated with the electronic brim which is able to adsorb thiophene (C_4H_4S) and facilitate a subsequent hydrogenation and C–S cleavage. This is an interesting observation since reactivity of MoS_2 structures has typically in the past been attributed to the presence of vacancies (see, e.g., [7]). The new insight indicates that the electronic edge states may play an equally important role, since they can donate or accept electrons just like ordinary catalytically active metal surfaces. The fact that the present results show that similar edge states exist for the hexagonal-like MoS_2 structures prevailing under sulfo-reductive conditions provides a new basis for addressing many questions in HDS. Further experiments with thiophene or other relevant probe molecules on the hexagon-like MoS_2 structures may give new insight on the metallic edges as active sites for hydrogenation and C–S bond cleavage.

The range of stability of the observed edge structures is evaluated in a thermodynamic model predicting the edge stoichiometries for the S edges and Mo edges, respectively. An important feature of the model is that it can be used to predict the state under real industrial HDS conditions. Interestingly, it is found that the S edge is expected to exist in the same configuration as found in the STM experiments, whereas for the Mo edge additional H atoms will saturate the monomer-covered edges under high-pressure and high-temperature conditions representative of HDS. It is therefore concluded that the MoS_2 clusters formed under the sulfo-reductive conditions of the STM experiment in many regards represent well the state of such clusters under real HDS conditions, and the model system is an excellent starting point for further studies of the many central questions that need to be solved in order to obtain a deeper understanding of HDS.

Finally, the present results also indicate that changing from one set of sulfiding environment does not readily result in structural interconversion once the MoS_2 clusters have been synthesized. Apparently, quite large activation barriers are involved in the structural transformations. Consequently, one may expect irreversible structural and morphological changes for industrial HDS catalyst activities. Activity measurements have provided support for such effects for promoted catalysts [7,64], and it is desirable to extend the present type of studies to the similar promoted HDS model catalyst [21] and investigate to which extent structural changes may also occur in the Co–Mo–S structures. It should be noted, however, that the present sulfiding conditions are quite different from the ones in industrial-type alumina-supported catalysts, where oxidic molybdenum structures are typically being sulfided [65,66]. In the future, the STM studies could also be extended to such type of model systems.

Acknowledgments

The authors gratefully acknowledge stimulating discussions with S. Helveg. This work was supported by the Danish Ministry of Science, Technology, and Innovation and by the Danish National Research Foundation through the Center for Atomic-scale Materials Physics (CAMP). J.V.L acknowledges support from the Danish Research Academy, the Interdisciplinary Center for Catalysis (ICAT), and the Danish Technical Research Council.

References

[1] I. Mochida, K. Sakanishi, X. Ma, S. Nagao, T. Isoda, Catal. Today 29 (1996) 185.
[2] D.D. Whitehurst, T. Isoda, I. Mochida, Adv. Catal. 42 (1998) 345.
[3] J.W. Gosselink, Cattech 4 (1998) 127.
[4] H. Topsøe, K.G. Knudsen, L.S. Byskov, J.K. Nørskov, B.S. Clausen, Stud. Surf. Sci. Catal. 121 (1999) 13.
[5] T. Kabe, A. Ishihara, W. Qian, Hydrodesulfurization and Hydrogenation—Chemistry and Engineering, Wiley–VCH, Kodansha, 1999.
[6] E. Derouane, Cattech 5 (2001) 214.
[7] H. Topsøe, B.S. Clausen, F.E. Massoth, Hydrotreating Catalysis, Science and Technology, Vol. 11, Springer, Berlin, 1996.
[8] R. Prins, V.H.J. de Beer, G.A. Somorjai, Catal. Rev.-Sci. Eng. 31 (1989) 1.
[9] B.S. Clausen, B. Lengeler, R. Candia, J. Als-Nielsen, H. Topsøe, Bull. Soc. Chim. Belg. 90 (1981) 1249.
[10] T.G. Parham, R.P. Merrill, J. Catal. 85 (1984) 295.
[11] S. Tauster, T. Pecoraro, R. Chianelli, J. Catal. 63 (1980) 515.
[12] H. Topsøe, R. Candia, N.-Y. Topsøe, B.S. Clausen, Bull. Soc. Chim. Belg. 93 (1984) 783.
[13] N.-Y. Topsøe, H. Topsøe, J. Catal. 139 (1993) 641.
[14] H. Topsøe, in: J. Bonnelle, B. Delmon, E. Derouane (Eds.), Proceedings of the NATO Advanced Study Institute on Surface Properties and Catalysis by Non Metals: Oxides, Sulfides and Other Transition Metal Compounds, Reidel, Dordrecht, 1983, p. 329.
[15] S. Kasztelan, H. Toulhoat, J. Grimblot, J. Bonnelle, Appl. Catal. 13 (1984) 127.
[16] R. Candia, B. Clausen, J. Bartholdy, N.-Y. Topsøe, B. Lengeler, H. Topsøe, in: Proceedings of the 8th International Congress Catalysis, p. 375.
[17] N.-Y. Topsøe, H. Topsøe, J. Catal. 84 (1983) 386.
[18] F. Besenbacher, I. Chorkendorff, B.S. Clausen, B. Hammer, A.M. Molenbroek, J.K. Nørskov, I. Stensgaard, Science 279 (1998) 1913.
[19] H. Over, Y.D. Kim, A.P. Seitsonen, S. Wendt, E. Lundgren, M. Schmid, P. Varga, A. Morgante, G. Ertl, Science 287 (2000) 1474.
[20] S. Helveg, J.V. Lauritsen, E. Lægsgaard, I. Stensgaard, J.K. Nørskov, B.S. Clausen, H. Topsøe, F. Besenbacher, Phys. Rev. Lett. 84 (2000) 951.
[21] J.V. Lauritsen, S. Helveg, E. Lægsgaard, I. Stensgaard, B.S. Clausen, H. Topsøe, F. Besenbacher, J. Catal. 197 (2001) 1.
[22] J.V. Lauritsen, M. Nyberg, R.T. Vang, M.V. Bollinger, B.S. Clausen, H. Topsøe, K.W. Jacobsen, E. Lægsgaard, J.K. Nørskov, F. Besenbacher, Nanotechology 14 (2003) 385.
[23] S. Helveg, PhD thesis, University of Aarhus, 2000.
[24] D. Broderick, G. Schuit, B. Gates, J. Catal. 54 (1978) 94.
[25] L.S. Byskov, B. Hammer, J.K. Nørskov, B.S. Clausen, H. Topsøe, Catal. Lett. 47 (1997) 177.
[26] L.S. Byskov, J.K. Nørskov, B.S. Clausen, H. Topsøe, J. Catal. 187 (1999) 109.
[27] L.S. Byskov, J.K. Nørskov, B.S. Clausen, H. Topsøe, Catal. Lett. 64 (2000) 95.
[28] P. Raybaud, J. Hafner, G. Kresse, S. Kasztelan, H. Toulhoat, J. Catal. 189 (2000) 129.
[29] L.S. Byskov, M. Bollinger, J.K. Nørskov, B.S. Clausen, H. Topsøe, J. Mol. Catal. A 163 (2000) 117.
[30] H. Schweiger, P. Raybaud, G. Kresse, H. Toulhoat, J. Catal. 207 (2002) 76.
[31] M.V. Bollinger, K.W. Jacobsen, J.K. Nørskov, Phys. Rev. B 67 (2003) 085410.
[32] S. Cristol, J.F. Paul, E. Payen, D. Bougeard, S. Clémendot, F. Hutschka, J. Phys. Chem. B 104 (2000) 11220.
[33] V. Alexiev, R. Prins, T. Weber, Phys. Chem. Chem. Phys. 3 (2001) 5326.
[34] S. Cristol, J.F. Paul, E. Payen, D. Bougeard, S. Clémendot, F. Hutschka, J. Phys. Chem. B 106 (2002) 5659.
[35] A. Travert, H. Nakamura, R. van Santen, S. Cristol, J. Paul, E. Payen, J. Am. Chem. Soc. 124 (2002) 7084.
[36] J.F. Paul, E. Payen, J. Phys. Chem. B 107 (2003) 4057.
[37] M.V. Bollinger, J.V. Lauritsen, K.W. Jacobsen, J.K. Nørskov, S. Helveg, F. Besenbacher, Phys. Rev. Lett. 87 (2001) 196803.
[38] E. Lægsgaard, F. Besenbacher, K. Mortensen, I. Stensgaard, J. Microsc. 152 (1988) 663.
[39] F. Besenbacher, Rep. Prog. Phys. 59 (1996) 1737.
[40] A.J. Leavitt, T.P.J. Beebe, Surf. Sci. 314 (1994) 23.
[41] J.V. Barth, H. Brune, G. Ertl, R. Behm, Phys. Rev. B 42 (1990) 9307.
[42] Dacapo pseudopotential code. URL http://www.fysik.dtu.dk/campos.
[43] K. Laasonen, A. Pasquarello, R. Car, C. Lee, D. Vanderbilt, Phys. Rev. B (1993) 10142.
[44] D. Vanderbilt, Phys. Rev. B 41 (1990) 7892.
[45] J. Perdew, J. Chevary, S. Vosko, K. Jackson, M. Pederson, D. Singh, C. Fiolhais, Phys. Rev. B 46 (1992) 6671.
[46] J. Tersoff, D.R. Hamann, Phys. Rev. Lett. 50 (1983) 1998.
[47] G. Wulff, Z. Kristallogr. 34 (1901) 449.
[48] W.K. Burton, N. Cabrera, F.C. Frank, Trans. R. Soc. A 243 (1951) 299.
[49] P. Raybaud, J. Hafner, G. Kresse, H. Toulhoat, Surf. Sci. 407 (1998) 237.
[50] K.K. Kam, B.A. Parkinson, J. Phys. Chem. 86 (1982) 463.
[51] T. Böker, R. Severin, A. Müller, C. Janowitz, R. Manzke, D. Voss, P. Krüger, A. Mazur, J. Pollmann, Phys. Rev. B 64 (2001) 235305.
[52] The identification was verified by testing many different edge configurations, which did not match the experimental findings; see Ref. [31]. We note that the edge states were found to exist independent of the Au(111) substrate. The major influence of the substrate is on the basal plane region which is rendered slightly conductive by interaction with Au.

[53] Note that DFT calculations for this configuration have recently indicated that the Mo edge atoms display a small pairing parallel to the edge [31]. However, due to the size of the applied unit cell this pairing cannot be achieved in the present calculations including a gold substrate. The energy associated with the pairing is small, estimated to 0.09 eV. Furthermore, the pairing is not reported for finite-sized Mo edges [30].
[54] J. Bachelier, J. Duchet, D. Cornet, Bull. Soc. Chim. Belg. 90 (1981) 1301.
[55] Y. Okamoto, Y. Katoh, Y. Mori, T. Imanaka, S. Teranishi, J. Catal. 70 (1981) 445.
[56] J. Valyon, R. Schneider, W. Hall, J. Catal. 85 (1984) 277.
[57] R. Burch, A. Collins, Appl. Catal. 17 (1985) 273.
[58] X.-G. Wang, A. Chaka, M. Scheffler, Phys. Rev. Lett. 84 (2000) 3650.
[59] K. Reuter, M. Scheffler, Phys. Rev. B 65 (2002) 035406.
[60] NIST Chemistry WebBook: NIST Standard Reference Database Number 69, July 2001 release, http://webbook.nist.gov/chemistry/.
[61] The presence of the Au substrate has not been included in the calculation for the S monomer + H configuration since this structure is not expected to be significantly perturbed by Au.
[62] J.V. Lauritsen, B.S. Clausen, H. Topsøe, F. Besenbacher, in preparation.
[63] Unlike the situation immediately after synthesis, the rest gas in this case contained no H_2S, thus excluding the possibility of extensive vacancy recombination with H_2S.
[64] R.P. Silvy, P. Grange, B. Delmon, Stud. Surf. Sci. Catal. 233 (1990).
[65] P. Arnoldy, J.A.M. van den Hiejkaut, G.D. de Bok, J.A. Moulijn, J. Catal. 92 (1985) 35.
[66] T. Weber, J.C. Muijsers, J.H.M.C. van Wolput, C.P.J. Verhagen, J.W. Niemantsverdriet, J. Phys. Chem. 100 (1996) 14144.